

Nano-hierarchical Hydrophobic Structure of Polycarbonate Fumed Silica Composites as a Thermal Barrier

Neha Katiyar¹, Neha Bhadauria¹

¹Department of Mechanical Engineering,

Krishna Institute of Engineering & Technology Ghaziabad

ABSTRACT

Recently, an intensive research effort has been devoted to the fabrication of polymer composites with enhanced thermal properties. This work proposes a thermal conductivity model and an inception pathway for the thermal analysis. Polycarbonate nano-composites filled Fumed silica (FS) was prepared by three different techniques viz. solvent casting, spray coating and melt blending. The results of morphology characterization indicated that FS particles are well dispersed in the polymer matrix. The thermal degradation behavior of composites was investigated by thermogravimetric analysis and also the thermal properties were investigated with respect to the thermal conductivity. The analysis for TGA chars entrenched the presence of alcoholysis reaction between PC and FS nanoparticles during thermal degradation. Therefore these melt blended composites have improved thermal insulation properties.

INTRODUCTION

Thermal conductivity plays a key role in heat transfer processes. As a matter of fact in many industrial applications, materials are selected primarily by considering their mechanical and thermal properties. In aerospace, power generation and automotive industries, materials like metal or ceramic matrix composites and porous ceramic thermal barriers are widely used for manufacturing the most advanced components. Now a days polymer matrix with inorganic fillers is competent with the other composites for the application of thermal insulation. The improvement of thermostability after incorporating the nanoparticles is due to the barrier network formed by nanoparticles and char hinders the transfer of volatile products and heat during the degradation process [1-2].

Polycarbonate (PC) nano-composites are attractive material for a range of industrial applications due to the unique properties that can be observed when compared to conventional composites. The incorporation of inorganic fillers into the polymer matrices was found to remarkably improve dimensional stability, and the mechanical, thermal, optical, electrical, and gas barrier properties, as well as to decrease the flammability [3-6].

Despite its excellent physical properties, the restriction on its thermal properties limits its application and workability. Some special applications involve electronic appliances, automobile, architecture and aerospace, and it is strongly desirable to improve the thermostability and flame retardancy of PC. Some research reports showed that the thermostability and flame retardancy of PC were reinforced after adding nano-inorganic fillers [7-11]. With the development of nanotechnology, recently various nano-size fillers as flame retardants, such as polyhedral oligomeric silsesquioxane, graphene, and montmorillonite [12-14] are turning into a new generation of high-performance fillers to meet industrial needs. As new class of flame retardants, inorganic nanoparticles are becoming a focus of both research and industrial applications. Fumed silica particles have also been used as fillers, polishing materials, pigments and reinforcement materials for its nonporous and hydrophobic characteristics [15-16]. Though, fumed silica is not listed as a carcinogen due to its fine structure; fumed silica can easily become airborne so utilizing it as filler is an environment benign. Fumed silica based thermal insulating composites have excellent thermal insulation properties [17-19]. Super critically dried silica aerogels and fumed silica compact have tantamount thermal conductivity [20-21]. Heat transfer at the nanoscale can differ distinctly from that predicted by classical laws [22]. Understanding nanoscale

heat transfer will help thermal management of electronic, optical, and optoelectronic devices, and design new materials with different thermal transport properties for energy conversion and utilization. Research on nanoscale heat transfer has advanced significantly over the past two decades, and a large number of interesting phenomena have been observed. In view of this characteristic, the composites are particularly useful in places where special heat insulation is demanded.

The present prospect deals with the critical strategy for the fabrication of inherently hydrophobic PC/NFS melt blended composite. In our previous work [23] we fabricated the PC/NFS thin film composite by a solvent-casting method and a spray-coating technique. Therefore in current work we are comparing the three processes *viz.* solvent casting, spray coating and melt blending in the view of PC/NFS composite and also with respect to difference characterizations. The main objective of present work is to develop an insulating composite having low thermal conductivity value and also to propose an analytical method to compute thermal conductivity which is supported by the experimental value of thermal conductivity. These composites embellished the insulation property over the car battery casing. The heat insulation adequacy and hydrophobicity of PC/NFS (unmodified) has not been much explored in literature. Yuezhan Feng et al. [24] were one of the early pioneers who understood the heat sinking capability of modified silica particles with char residue at approximately 35% but in the present report we show an improved thermal behavior with 70% char residue without surface modification of fumed silica particles. The heat sinking capability of the present patterns opens new horizons in technologies involving high temperature fluids. They can be effectively used in the car battery casing to insulate it and its application can also be extended in the field of aircraft heat insulating tiles and also as a base layer of thermal and electrical insulating material in heating units. This composite represents the best combination of heat sinking with adequate hydrophobicity and making it an ideally suitable candidate in the automotive industry as well as in the electronic industry.

Experimental procedure

Materials and synthesis

Polycarbonate (SABIC Innovative Plastics India Pvt. Ltd, India, LEXAN grade 143R, viscosity 22 cP, MFI $\frac{1}{4}$ 10.5 g per 10 min) was used for the preparation of composites. Fumed silica nanoparticles, 99.8% pure silica, $200\text{m}^2\text{g}^{-1}$ of surface area, 2.3 g cm^3 of density and particle size varies from 7 nm to 14 nm, according to the manufacturer, was purchased from Sigma Aldrich Corp., USA. All reagents and solvents involved were of analytical grade and were used without any further purification.

Fabrication of PC/NFS composite

Composite membranes of a continuous polymer matrix and a well dispersed filler phase have appealing potential in various fields including the automotive industry, military applications and electronic industry. The characteristics of composite provide more degrees of freedom to accommodate a multiscale structure and integrate multiple functionalities compared to pristine polymer membranes. In the past two decades, a variety of fabrication methods for composite membranes have been explored, e.g. physical blending method, sol-gel method, infiltration method, in situ polymerization method, interfacial polymerization method, chemical atomic layer deposition method, layer by layer assembly method, etc [29-30] In the present paper we have delineated and compared three optimized techniques, *viz.* solvent casting, spray coating and melt blending, for the fabrication of heat insulating composites and studied properties for their applications in car battery casings. The solvent casting and spray coating method had been covered in our previous article [23]. The melt blending method for the preparation of PC/NFS composite has been chronicled subsequently.

Melt Blending of composite

The particulate composites of PC/NFS were prepared by the melt extrusion of polycarbonate. The fumed silica particles used for the blending purpose were first sieved through a 45mm sieve. The polymer was dried in an air circulated oven at 120–140°C for 2h prior to blending. A sample is

prepared with 30 wt% fumed silica in the polymer matrix. A fully intermeshing co-rotating twin screw extruder was used for extrusion with a screw diameter of 20 mm and a 40:1 L/D ratio. Co-rotating screw extruders usually have a uniform shear rate distribution in the segmented screw sections and attainment of distributive mixing of filler particles in the polymer matrix [31-32]. The pre-dried polymer and NFS compound were extruded through a circular die with a diameter of 50 mm with operating conditions at 280°C and rpm in the range of 20–25. Once the blends were extruded, they were water cooled, pulled and pelletized with the help of a pelletizer. The pelletized granules of PC/NFS composite were pre dried at 90±5 °C for 12 h and conditioning was done at 23–27 °C for 24 h prior to characterization as depicted in Fig 1.

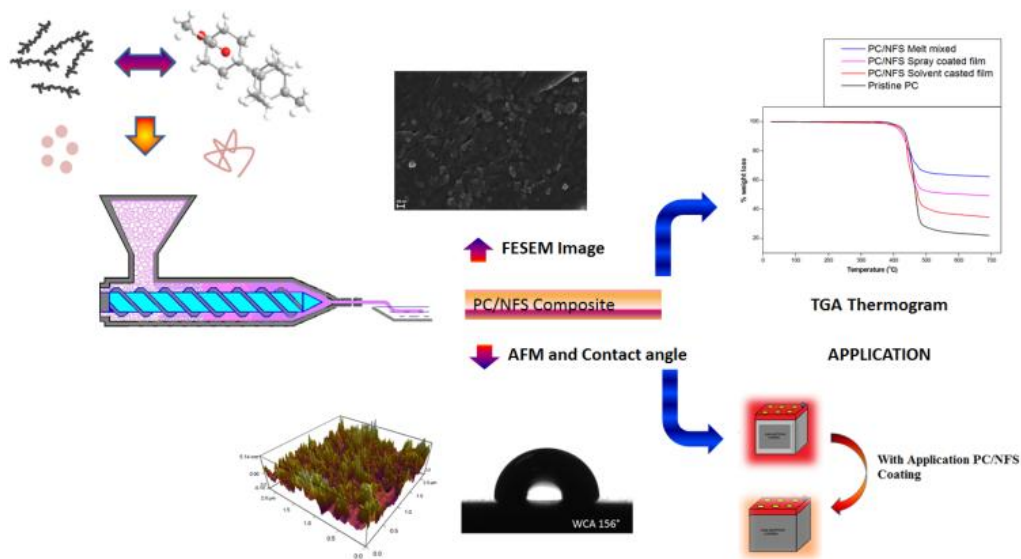


Fig 1. Graphical representation of melt blending technique of PC/NFS composite

Characterization techniques

The morphologies of the PC/NFS composite were observed by FESEM with an accelerating voltage of 5.00 kV and high resolution transmission electron microscopy (HRTEM) images were acquired operated at 300 kV. Surface roughness of samples were depicted using AFM (Asylum research, an oxford instrument company, UK) in tapping mode and the water contact angle (WCA) measurements were carried out on a Krüss DSA100 (Germany) contact angle goniometer using deionised water at ambient temperature. The FTIR spectrum was monitored and compared for pristine PC as well as for PC–NFS composite. The spectrum was chronicled between 4500 and 500 cm^{-1} at room temperature on PerkinElmer Spectrum BX FTIR system (PerkinElmer Inc., USA). Thermogravimetric analysis (TGA) was performed on a thermogravimetric analyser TGA/SDT A851e Mettler Toledo (USA). The heating rate was set to 5 $^{\circ}\text{Cmin}^{-1}$ under inert N_2 atmosphere and the analytical temperature region was set from ambient temperature to 800 $^{\circ}\text{C}$.

Morphological Analysis

The obtained nano fumed silica particles were characterized using FESEM and HRTEM. The FESEM image of NFS particles depicts their three-dimensional nanoscale chain-like morphology. The inherent chain-like structure of fumed silica spherical nanoparticles and bridging structure⁶⁵ was also reaffirmed from an HRTEM micrograph as described in our previous article. In contrast to the morphology of solvent casted and spray coated films as discussed in our previous work [23], in present prospect the FESEM images of pristine PC and PC/NFS melt blended composite exhibit more dispersion of fillers as shown by Fig.2.

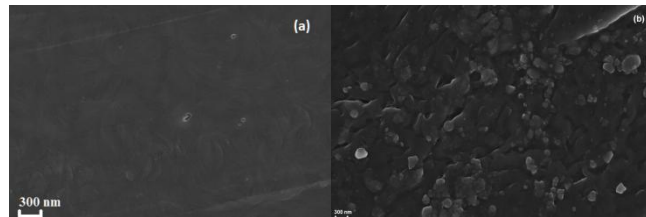


Fig 2 FESEM images of (a) Pristine PC (b) PC/NFS blend composite

Compositional and Functional Group Analysis

Fourier Transform Infrared (FT-IR) analysis

To understand the interactions between PC and NFS, the FT-IR absorption spectra of PC, pure NFS and PC/NFS were acquired and compared as shown in Fig. 3. The characteristic peaks of PC located at 1152, 1188 and 1227 cm^{-1} as an intense triplet were due to the strongest infrared absorptions in polycarbonate and are due to the C–O single bond stretches and aromatic ring breathing modes. Meanwhile the formation of new peaks at 1094 cm^{-1} and 3821 cm^{-1} in PC/NFS composite indicate the interaction between them and can be assigned to the O–Si–OH deformation mode and absorption peak of methylene stretching vibration respectively [33-34]. The free surface of hydroxyl groups –SiOH appear as peaks at 1772 cm^{-1} and 3742 cm^{-1} [35-36]. The inexistence of these peaks in the FT-IR spectrum of pristine PC positively suggests the exquisite interaction between the PC and NFS particles and also the presence of (–C)O formed by the pyrolysis of (–CO₃) group.

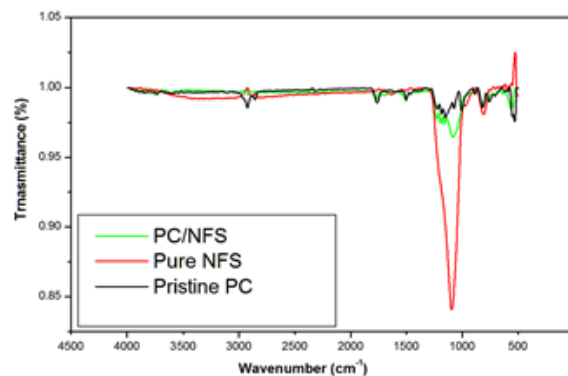


Fig 3 FT-IR spectra of NFS, pristine PC and PC/NFS (10 wt%).

Topographical analysis and contact angle measurement

The increase in the roughness of the coating on incorporation of fumed silica was clear from the roughness studies. The roughness profiles taken for the PC coating and the PC/NFS composite coating with 30 wt% fumed silica is shown in Fig.5. Pristine PC coating exhibited low surface roughness with an average roughness (Ra) of 4.5 nm. The AFM analysis of pristine PC, solvent casting and spray coating was described in our previous article [23]. Fig 4 shows the PC/NFS composites which represent the spike like morphology are the most advantageous for tolerating the impact of collision with surface roughness of 15 nm [37]. Surface roughness is an inexorable, ordinary phenomenon that tends to increase the surface reactivity, stimulates turbulent transitions of heat flow causing a shoot in the surface recession [38-40] which validate PC/NFS composite is most feasible for thermal appliances that produces extreme dissipation of heat.

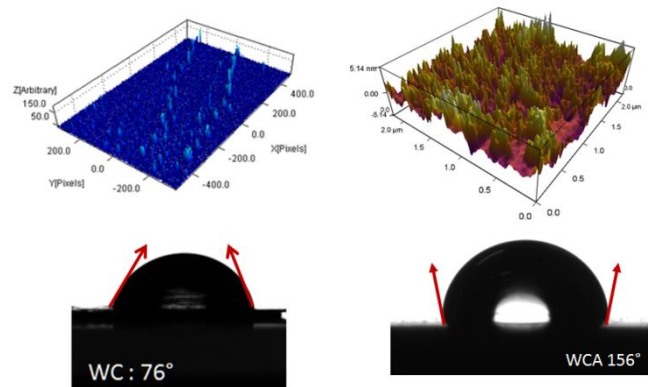


Fig 4 AFM and contact angle measurement for Pristine PC and PC/NFS composite

Wettability study of pristine PC and PC/NFS composites was examined by measuring the contact angle of sessile drops as mentioned in our previous article for solvent casted and spray coated films [23]. The water contact angle for PC/NFS composite fabricated by melt blending has been shown in Fig 4. Balasubramian K et al. and other researchers have thoroughly explored in their studies that contact angle predominantly depends on the surface roughness of the substrate based on the Cassie–Baxter model [41,42]. In the disparity to the Wenzels and Cassie–Baxter model Gao et al. reported that the contact angle of sessile drop on solid surface depends on the three phase contact line formed due to the perpetuation of the drop on surface instead of surface roughness under the contact area [43–46].

McCarthy model implies that, the wetting characteristics of any solid surface endowed to be the three phase contact line pinning which results in measurable contact angle between spheres and solid surface and subsequently depend on the surface topology under the area of the contact line. In this context, the surface roughness value determined by the SPIP software exhibited acceptable resemblance with the McCarthy model. There is a progressive increment in the surface roughness value of the PC/NFS coating. The enhanced surface roughness value and contact angle was noticed which may be due to the uniform dispersion of the fumed silica particles in the PC matrix. The roughness values for the samples fabricated by the solvent casting and spray coating are 6.3nm and 12nm respectively as mentioned in the previous article also while in current work the roughness value is calculated as 15nm for the melt blended composite. This consequential increment in the PC/NFS composite as compared to pristine PC is might due to the consistent dispersion of the fumed silica in the PC matrix.

Thermogravimetric Analysis

It was speculated that the insulation of PC containing Fumed silica is caused by accelerating the thermal degradation rate of PC to ensure the formation of an insulating carbon layer on the surface that inhibits the supply of flammable gas and heat transfer [47–48]. When the thermal energy begins to surpass the bond energies of various bonds in the PC chains, a random chain scission takes place and the degradation rate rapidly increases. It is apparent that the lowest bond energies are 251 and 330 kJ mol⁻¹ and these are assigned to the C–C bond of isopropylidene and the C–C bond of carbonate, respectively [49]. The influence of tiny amounts of individual additive on the thermal degradation of PC was examined.

Fig. 5 shows the decomposition thermographs of PC/NFS composites. All the curves depict a single stage degradation pattern. The thermographs can be divided into three major zones: the first reaction zone (25–360 °C), where water, un-reacted oligomers and small groups such as methane, ethylene acetone are evaporated. In the second stage (350–480 °C), initial decomposition occurs at 350 °C, determining the onset of pyrolysis of the polymer. Over this zone, weight loss occurs because of

thermal decomposition during pyrolysis. In the third zone (480–700°C), as there is FS filler in the PC matrix incremental increase in the thermal stability of the composite is observed. The augmentation in thermal stability may be attributed to the restricted mobility of segmental movement of PC molecular chains, which is due to the enhanced interaction between FS and the polymeric matrix. Restriction of the mobility of the polymer chains by oxide particles present in FS also contributes to the improvement observed in thermal stability [50].

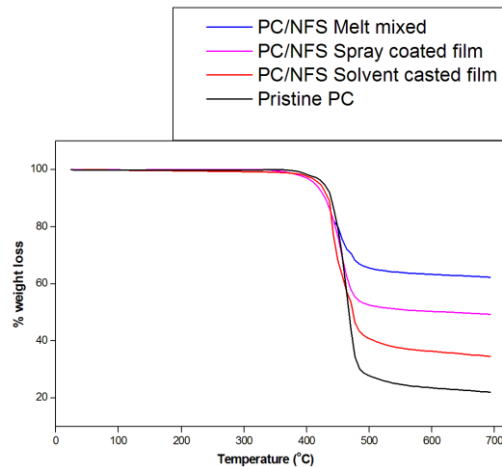


Fig 5. TGA thermograph of PC and PC/NFS composites

The comparison of three techniques viz. solvent casting, spray coating and melt blending has been done with same wt% of the filler in terms of char residue and integral procedural decomposition temperature which indicates the thermal stability of the composite. Tailored properties of composite have been ascertained by altering the fabrication process which can be reaffirmed by different analysis described as below.

Integral procedural decomposition temperature (IPDT)

The integral procedural decomposition temperature (IPDT) is utilized to evaluate the thermal stability of the PC/PNFS composite [51]. Some other researcher had also utilized the IPDT analysis for the establishment of thermal stability [52-54]. The formula used for computation was:

$$IPDT(^{\circ}C) = A \times K \times (T_f - T_i) + T_i \tag{1}$$

Where, $A = \frac{S_1 + S_2}{S_1 + S_2 + S_3}$ (2)

$$K = \frac{S_1 + S_2}{S_1} \tag{3}$$

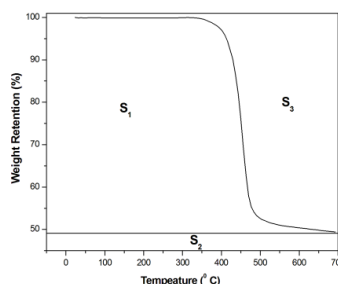


Fig6. Schematic representation of S₁, S₂ and S₃, which are used to obtain A and K

Where A is the area ratio of the TGA thermogram, T_i is the initial and T_f is the final experimental temperature. Fig 6 represents the schematic of S_1 , S_2 and S_3 , which are surface areas related to TGA thermogram and useful for the determination of A and K value as mentioned in equation 2,3. The IPDT of pristine polymer was 710 °C and for composite is described in Table 1.

Table 1. Thermal characteristics of PC/NFS composites

Serial No.	Sample Name	Residue (%) at 700 °C	IPDT (°C)
1	Pristine PC	22	710
2	PC/NFS 30 wt% (Solvent)	38	1027
3	PC/NFS 30 wt% (Spray)	49	1436
4	PC/NFS 30 wt% (Melt)	61	2215

In view of the Table 1, the IPDT values of composites are higher than that of pristine polymer. The higher IPDT values signify that NFS contributes in the formation of carbon layer on heating in nitrogen atmosphere, composed of silica encompasses a substantial amount of free-carbon. Substantial increment in the values of IPDT manifest that there is enhancement in the thermal stability of the PC/NFS composite. Therefore it is conspicuous that inorganic elements can hike the thermal stability of polycarbonate.

Thermal Conductivity analysis

As previously mentioned thermal conductivity plays paramount role in the field of thermal insulation of the materials. Maxwell identified the first theoretical model for thermal conductivity of a two phase system by considering spherical fillers dispersed in a continuous matrix. Maxwell also assumed that these filler particulates had no thermal interaction with each other [55]. The spherical geometry of the NFS particles supports the Maxwell model for the calculation of thermal conductivity for the present work as well as we mentioned in our previous article. In present prospect our aim to validate the theoretical result with the experimental result of thermal conductivity. As in the theoretical model of the Maxwell, as there was many assumptions made by him. Due to the difference between assumptions and real conditions in the measurement in the thermal conductivity, there is disparity between the calculated and experimented values as explicated in Table 2. The thermal conductivity was calculated with the Maxwell formula as explained in the previous article [23].

Serial No.	Sample Name	Thermal conductivity (Calculated) W/m°C	Thermal conductivity (Experimental) W/m°C
1	Pristine PC	0.19	0.19
2	PC/NFS(Solvent)	0.14	0.18
3	PC/NFS (Spray)	0.13	0.16
4	PC/NFS (Melt)	0.12	0.17

Table 2. Thermal conductivities values of composites

Thermal Degradation Mechanism

For assuring the possible degradation reaction between PC and NFS particles, the chemical structure of the char residues was analysed by FTIR. As shown in Fig.7 the characteristic peaks of the chars for both composites are similar to those of neat PC except the broad band at 1000-1250 cm^{-1} . The difference between neat PC and its composites at 1000-1250 cm^{-1} is attributed to the presence of Si-O bond [56]. In comparison with the IR peak of Si-O in pristine SiO_2 (1100 cm^{-1}), the peak position of Si-O in char residues for both composites shifts to 1110 cm^{-1} for both composites. This result may be ascribed to the asymmetry stretching vibration of C-Si-O, which is produced by the alcoholysis reaction between PC and silica nanoparticles.

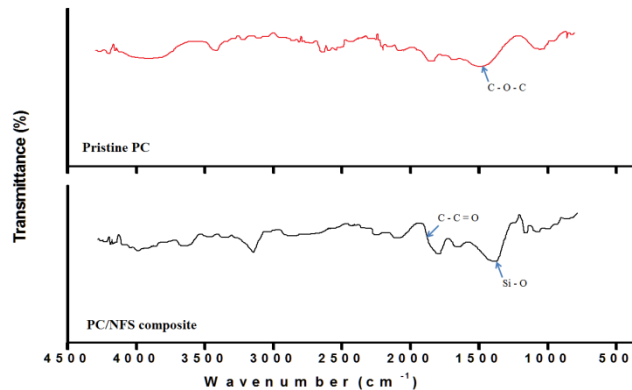


Fig 7 FT-IR spectra of TGA char residues

Conclusion

The commenced study describes the hydrophobic characteristics with enhanced thermal insulation demeanor of PC/NFS composites. It also elucidate the thermal degradation behaviour of PC/NFS nano-composite, prepared by melt blending, was systematically explored in nitrogen atmosphere and subsequently correlates with the other two techniques viz. solvent casting and spray coating as discussed in our previous article. The char residue of PC has a significant improvement after incorporating pristine fumed silica nanoparticles. The thermal insulation behaviour of composites had also reaffirmed with the experimental values of thermal conductivity. In contrast of all the three processes with respect to the thermal insulation behaviour, we obtain the best tailored properties of composite fabricated by melt blending. In addition the application of PC/NFS composite can be easily extended in the field of high temperature application with hydrophobic properties.

References

- [1] Y. Badhe and K. Balasubramanian, RSC Adv., 2014, 4, 28956.
- [2] Y. Badhe and K. Balasubramanian, RSC Adv., 2014, 4, 43708.
- [3] P. C. Ma, N. A. Siddiqui, G. Marom and J. K. Kim, Composites, Part A, 2010, 41, 1345.
- [4] H. Zou, S. Wu and J. Shen, Chem. Rev., 2008, 108(9), 3893.
- [5] R. Sengupta, M. Bhattacharya, S. Bandyopadhyay and A. K. Bhowmick, Prog. Polym. Sci., 2011, 36(5), 638.
- [6] S. Sinha Ray and M. Okamoto, Prog. Polym. Sci., 2003, 28(11), 1539.
- [7] M. Rahil Parvaiz, P. A. Mahanwar, S. Mohanty and S. K. Nayak, J. Miner. Mater. Charact. Eng., 2010, 9(11), 985.
- [8] S. C. Moon, J. Y. Kim and B. T. Oh, Polym. Eng. Sci., 2014, 54(6), 1289.
- [9] R. Poerba, M. Spirkova and Z. Hrdlicka, Process. Appl. Ceram., 2011, 5(3), 155–159.
- [10] H. R. Hakimelahi, L. Hu, B. B. Rupp and M. R. Coleman, Polymer, 2010, 51, 2494.
- [11] P. Jindal, M. Goyal and N. Kumar, Mater. Des., 2014, 54, 864.
- [12] L. Song, Q. He, Y. Hu, H. Chen and L. Liu, Polym. Degrad. Stab., 2008, 93(3), 627.
- [13] G. Gedler, M. Antunes, V. Realinho and J. I. Velasco, Polym. Degrad. Stab., 2012, 97(8), 1297.
- [14] J. Feng, J. Hao, J. Du and R. Yang, Polym. Degrad. Stab., 2010, 95(10), 2041–2048.
- [15] M. Ettlinger, T. Ladwig and A. Weise, Prog. Org. Coat., 2000, 40, 31.
- [16] V. M. Gun'ko, E. F. Voronin, E. M. Pakhlov, V. I. Zarko, V. V. Turov, N. V. Guzenko, R. Lebeda and E. Chibowski, Colloids Surf., A, 2000, 166, 187.
- [17] J. P. Feng, D. P. Chen, W. Ni, S. Q. Yang and Z. J. Hu, J. Non-Cryst. Solids, 2010, 356, 480–483.
- [18] H. Abe, I. Abe, K. Sato and M. Naito, J. Am. Ceram. Soc., 2005, 88, 1359.

- [19] M. Naito, A. Kondo and T. Yokoyama, *J. Iron Steel Res. Int.*, 1993, 33, 915.
- [20] J. Fricke and T. Tillotson, *Thin Solid Films*, 1997, 297, 212.
- [21] Z. S. Deng, J. Wang and A. M. Wu, *J. Non-Cryst. Solids*, 1998, 225, 101.
- [22] G. Chen, *Nanoscale energy transport and conversion: a parallel treatment of electrons, molecules, phonons, and photons*, Oxford University Press, 2005.
- [23] Neha Katiyar, Balasubramanian K. *RSC Adv.*, 2015, 5(6), 4376-4384.
- [24] Y. Feng, B. Wang, F. Wang, Y. Zhao, C. Liu, J. Chen and C. Shen, *Polym. Degrad. Stab.*, 2014, 107, 129.
- [25] B. P. Tripathi and V. K. Shahi, *Prog. Polym. Sci.*, 2011, 36, 945.
- [26] B. Lin, S. Cheng, L. Qiu, F. Yan, S. Shang and J. Lu, *Chem. Mater.*, 2010, 22, 1807.
- [27] H. Wu, B. Tang and P. Wu, *J. Phys. Chem. C*, 2010, 114, 16395.
- [28] S.-M. Lee, V. Ischenko, E. Pippel, A. Masic, O. Moutanabbir, P. Fratzl and M. Knez, *Adv. Funct. Mater.*, 2011, 21, 3047.
- [29] M. A. Priolo, K. M. Holder, D. Gamboa and J. C. Grunlan, *Langmuir*, 2011, 27, 12106.
- [30] H. Althues, J. Henle and S. Kaskel, *Chem. Soc. Rev.*, 2007, 36, 1454.
- [31] B. D. Favis and D. Therrien, *Polymer*, 1991, 32(8), 1474.
- [32] F. Goffreda, A. Griff, L. Livinghouse, T. Walsh and J. Scuralli, *Tool and Manufacturing Engineers Handbook Knowledge Base*, Society of Manufacturing Engineers, 1998.
- [33] S. Go, M. Han and Y. Ahn, *Bull. Korean Chem. Soc.*, 2012, 33(11), 3899.
- [34] *The Surface Properties of Silica*, ed. A. P. Legrand, Wiley, New York, 1998.
- [35] J. B. Beziger, S. J. McGovern, B. S. H. Royce, *ACS Symposium Serial*, 1985, 288, 449.
- [36] F. Buccuzzi, S. Coluccia, G. Ghiotti, C. Morterra and A. Zecchina, *J. Phys. Chem.*, 1978, 82, 1298.
- [37] C. Mundo, M. Sommerfeld and C. Tropea, *Int. J. Multiphase Flow*, 1995, 21, 151.
- [38] C. D. Stow and M. G. Hadfeld, *Proc. R. Soc. London*, 1981, A373, 419.
- [39] C. Escure, M. Vardelle and P. Fauchais, *Plasma Chem. Plasma Process.*, 2003, 3, 291.
- [40] R. F. Allen, *J. Colloid Interface Sci.*, 1975, 51, 350.
- [41] M. Q. Zhang, M. Z. Rong, H. M. Zeng and K. Friedrich, *J. Appl. Polym. Sci.*, 2001, 80, 2218.
- [42] B. Nanda Sahoo and B. Kandasubramanian, *RSC Adv.*, 2014, 4, 220.
- [43] L. Gao and T. J. McCarthy, *Langmuir*, 2006, 22, 6234–6237.
- [44] L. Gao and T. J. McCarthy, *Langmuir*, 2007, 23, 3762–3765.
- [45] L. Gao and T. J. McCarthy, *Langmuir*, 2007, 23, 13243.
- [46] L. Gao and T. J. McCarthy, *Langmuir*, 2009, 25, 14105–14115.
- [47] A. Ballistreri, G. Montaudo, E. Scamporrino, C. Puglisi, D. Vitalini and S. Cucinella, *J. Polym. Sci., Part A: Polym. Chem.*, 1988, 26(8), 2113.
- [48] J. L. Koenig, *Spectroscopy of polymers*, Elsevier, 1999.
- [49] S. Baglari, M. Kole and T. K. Dey, *Indian J. Phys.*, 2011, 85(4), 559.
- [50] N. Katiyar and K. Balasubramanian, *RSC Adv.*, 2014, 4, 47529.
- [51] Chung-Hwei Su & Yi-Pang Chiu & Chih-Chun Teng & Chin-Lung Chiang, *J Polym Res.*, 2010, 17, 673–681.
- [52] C.D. Doyle, *Anal. Chem.*, 1961, 33(1), 77-79.
- [53] Fan-Long Jin, Soo-Jin Park, *Polym. Degrad. Stab.*, 2012, 97(11), 2148-[56] Zhi Li, Ping Wei, Ying Yang, Yonggang Yan and Dean Shi, *Polym. Degrad. Stab.*, 2014, 110, 104-112.
- [54] M. James Clark, *Electricity and Magnetism*, Clarendon Press, Oxford, 1873.
- [55] Alok Agrawal, Alok Satapathy, *Universal Journal of Mechanical Engineering*, 2015, 3(1), 1-6.
- [56] Wawrzyn E, Schartel B, Seefeldt H, Karrasch A, Jäger C. *Ind Eng Chem Res* 2012; 51(3): 1244-55.